COMPUTER SUPPORT FOR PRESSURE DISTRIBUTION CONTROLLED SHAPE DESIGN

C.C.M. Moes, M.Sc.
Delft University of Technology, the Netherlands

ISATA: 99ME068

Keywords: *Design for ergonomics, point cloud modelling, fuzzy shape conceptualization, consideration of pressure distribution, shape compensation function, spatial lattice model.*

1 INTRODUCTION

Cars and vehicles are typical products that are in daily, direct and constant interaction with domains of the human body when in use. These products are manipulated with the hands or feet (control-arms, pedals), support the body (seats, beds), or provide protecting function (cabins, safety devices). In order to increase the comfort of use, designers should strongly consider ergonomic factors besides functionality and aesthetics when conceptualizing the shape of these units and components. An obvious problem is that the current generation of CAE programs, that are used by product designers to model the geometry and the physical behaviour takes no care of the ergonomical aspects of the user groups. The objective of our research has been to develop computer support for shape conceptualization by consideration of the body characteristics of a specific user group and the contact pressure distribution. Besides the elaboration of the computer algorithms and tools, which is the main topic of this paper, our research had to be concerned also with formalization of the requested ergonomics knowledge.

The involvement of pressure distribution in the conceptualization of the optimum shape of the contact areas of products, goes together with the need for a new type of modelling, which allows for the simultaneous consideration of modality, vagueness and incompleteness. The modality originates in that more than one subject, product instance and relationship have to be covered by the computer oriented methodology. Since the aforementioned products are manufactured in large series the statistical distributions of the body characteristics of the user group have to be considered. The product instances have to be derived based on incomplete pressure distribution, dimensional and deformation data. Thus, to solve the problem fuzzy engineering is needed.

This paper describes the specific algorithms that are needed for the computer supported pressure controlled conceptualization of the product shape, with a focus put on sitting supports.

2 PROBLEM STATEMENT AND RELATED RESEARCH

Figure 1 gives an overview of the problem components to be solved and worked out. The idea is (i) to measure the pressure distribution of subjects sitting on a flat, hard and horizontal support, and to express these pressure data in a set of fuzzy parameters. The measurement substrate is not a curved surface because an unreasonable would be required for different curvatures, different subject, and varying posture. Now the flat pressure distribution data will be applied to the fuzzy described unloaded body, followed by a compensation procedure for unacceptable high pressure values. The next step is (ii) to obtain the relevant anatomical and mechanical characteristics of the pelvic area, and again to convert these data into a set of fuzzy variables, (iii) to assess the physiological, biomechanical and anatomical criteria for the pressure that is exerted in the skin and is transmitted via the body, and (iv) to apply the pressure distribution on the shape of the unloaded body. Since all variables are fuzzily described, this application requires an according number of passes of FEM programs. The result is a deformed body, with a ‘more or less’ flat outward shape. Since the pressure distribution is

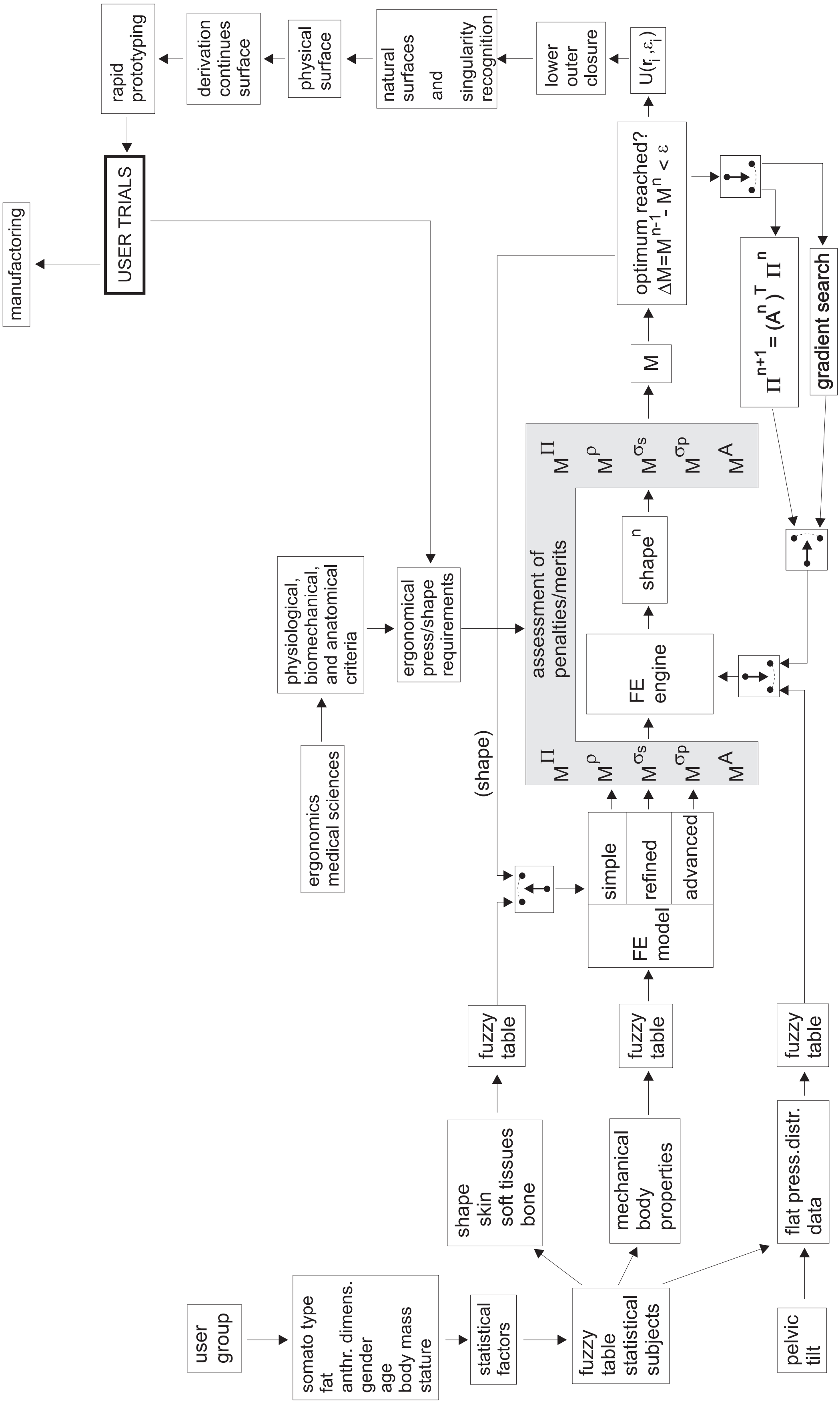

Fig 1. Schematic view of the procedures and the algorithms

measured on a flat support, it usually results in two pressure peaks. In most cases this pressure tends to exceed the physiologically acceptable limits [1, 2]. Therefore the shape must be modified to correct for such pressure values. This is again obtained by dedicated FEM techniques. The average pressure in the contact area is an indicator for the maximum attainable improvement. The shape modification results in a change of the *magnitude* of the contact area, so that the average pressure decreases the users' discomfort, or in a change of the *shape* of the contact area, which enforces a shift of the pressure patterns. The new shape is represented as a fuzzy cloud of shape defining points, which are described as a set of position vectors with the related metric occurrences. The resultant point cloud is (v) converted to a physical shape and a continuous surface via singularity recognition, natural surface recognition, and mathematical specification of the smooth surface patches [3, 4]. Finally, (vi) a prototype of the surface is subject to user trials, which always constitute the absolute final decisive control whether the result is ergonomically sufficient.

Physiological, biomechanical and anatomical criteria in relation to sitting are discussed in [1, 5, 6, 7, 8, 9]. Data on the capillary blood pressure were already long ago reported by [10]. An extensive study on product factors that relate to the ergonomics of sitting comfort can be found in [11]. Studies on mechanical properties, mechanical FE models of the pelvic region, and on the transfer of mechanical load to human tissue were reported by [12, 13, 14, 15]. Results of pressure distribution measurements and the registration of the angle of the pelvic tilt can be found in [2, 16]. An review of literature on the tissue shape and the deformation versus the applied pressure distribution is given in [17]. The design relevance of the current project, the assessment of an ergonomically acceptable product shape, has been discussed for different product groups in many standard works on ergonomics (but none of such methods are based on an intelligent computer support other than the usual CAD systems). The mathematical fundamentals for the conversion of the obtained point cloud, via the recognition of singularities and natural surfaces, into a physical surface and, finally, the construction of a continuous surface by rapid prototyping was reported in [4, 3, 18]. User trial procedures have been described in many books on ergonomics and ergonomics methodologies, for instance [19, 20].

3 KNOWLEDGE OF THE BODY- AND THE PRESSURE DATA

Since the algorithms make extensive use of the finite elements methods, first the shape and the mechanical characteristics of the buttock region must be represented by a set of Fe models, see figure 1(ii), followed by the measured pressure distribution data, see figure 1(i). The characteristic spatial and mechanical data of a FE model of the buttock region are defined by (i) the shape of the outer surface and of the internal continuum, (ii) the mechanical properties of the body, and (iii) the angle of the pelvic tilt.

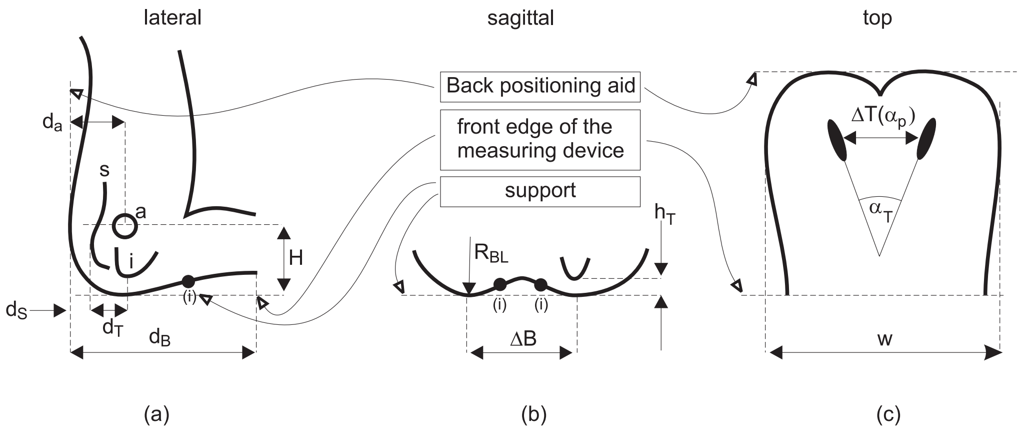

Fig 2. The shape descriptors of the human pelvic area for an upright sitting person. In figure (a) represent 's', 'a' and 'i' the sacrum, the acetabulum, and the ischial tuberosities respectively.

Shape descriptors of the unloaded buttock region

The important dimensions can be seen in figure 2a, b and c. Figure 2a shows the body components in a lateral view. The sagittal projections on the midsagittal plane of the sacrum (s), the ischial tuberosities (i), and the acetabulum (a) are indicated. Figure 2b shows the dorsal view with the sacrum, the iliac bones and the ischial tuberosities. R_{BL} is the lateral curvature of the lower skin surface of the buttocks. The sagittal curvature R_{BS} is not shown. The curvature inflections points for the respective cross section are indicated as (I). The curvatures, R_{TL} and R_{TS}, of the ischial tuberosities are also not shown. An important measure with respect to the maximum impression is the vertical distance, h_T, between the ischial tuberosities and the skin. ΔB is the lateral distance between the lower aspects of the skin. Figure 2c shows the top view. The important measure in this subfigure is the distance between the lower aspects of the ischial tuberosities. Since they show an angle of inclination towards each other in the sagittal direction, a lateral (around a lateral axis) pelvic rotation induces a change of this distance, so that $\Delta T = f(\alpha_p)$, where α_p is the angle of the pelvic tilt. It depends on the angle of inclination, α_T, and on the curvature of the tubs. These measures constitute the main variables for the spatial aspects of the FE model of the buttock area. Some of them were investigated in [21, 2, 22, 16].

Mechanical properties of the unloaded buttock region

The mechanical characteristics for a FE model include (i) the elastic properties (Young's modulus), (ii) the compressive properties (bulk modulus and Poisson's ratio). Estimated values are found in [12], (iii) the viscous properties, and (iv) the connective strength of the different body parts e.g., of the skin and the ischial tuberosities. The intra-individual anthropometric variability introduces fuzziness into the modelling of FE models. Since FE-machines can not handle fuzzy defined elements, the fuzzy models and pressure distribution-data are represented by a number of percentiles in a statistical table. The main factors, that describe 69% of the variability of the subjects (healthy students), are (i) the somatotype, and (ii) gender [2]. These factors must be used to compile the experiment design table for the application of the pressure distribution on a set of 'statistical subjects', which are defined by a set of percentiles of the factors. The table contains $N_C = n_F \times n_P$ cells, where N_C is called the number of cases, that will be analyzed, where n_F is the number of factors and n_P the number of percentiles. Each cell, $\mathbf{S}_j^0$ $(j = 1, \ldots, N_C)$, of the table contains (i) a set of spatial points of the finite elements, (ii) the mechanical properties. Thus, the table contains a set of imaginary bodies that together statistically cover the user group, instead of a set of human individuals.

4 CALCULATION MODELS

This section introduces the procedure in more detail.

4.1 Considerations for a FE model of the buttock area

FE-machines can process only sharply defined elements. The set of FE-models for the current research must therefore be derived from the percentilized statistical data of the body (the above mentioned statistical table).

A relatively simple model of the unloaded body distinguishes between the hard, bony tissue showing high E, and the soft tissues with low E and, since the body contain mainly water, high bulk modulus B. Consequently is the Poisson's ration $\nu \approx 0.5$. The internal shear as well as the shear within the contact area are ignored. The soft tissue must be surrounded by a sort of skin to prevent the falling apart of the soft continuum. The tubers are modelled as half spheres, mounted at the lower aspect of a vertical cylinder (intended to represent the upright posture). They are positioned at a certain height with respect to the skin below. The skin is also modelled as a half sphere with corresponding radius.

An advanced model commences from this simple model. The following modifications are then incorporated. (i) The skin has more realistic properties(anisotropic E, ν, viscosity), (ii) the model of the bony pelvis resembles a real pelvis, (iii) the soft part consists of different tissues with its specific constituents (muscles, adipose tissue, dermis, epidermis), (iv) the outward shape of the pelvic model, which can be obtained with e.g., laser scanning techniques, is more natural, (v) the upper legs are included, (vi) internal shear and (vii) shear in the contact areaare considered, the connective strength of the ischial tuberosities and the skin or the soft tissues is controlled. Moreover, models are constructed for varying pelvic tilt.

Depending on the available knowledge and methodologies various intermediate models can be defined, which are indicated as 'refined' in figure 1.

4.2 Measurement and representation of the fuzzy pressure distribution

A more detailed description of the measurement (on a flat, horizontal surface) and the representation of the pressure distribution data were reported earlier [23, 24, 25]. For the current context the pressure distribution must be expressed as a vector-vector function. The position vector, **a**, points to a location in $\Re^3$. The set of these locations is described as the surface lattice with indices in the x- and y-direction, $\mathbf{A} = \{\mathbf{a}_{i,j}\}$ $(i = 1, \ldots, N_x; j = 1, \ldots, N_y)$. N_x and N_y are the numbers of 'rows' and 'columns' of the measuring device. In the following the double indexing (i, j) will be replaced with one running index $k = (i-1)N_y + j$. The maximum value of k is thus number of measuring elements $N_L = N_x \times N_y$. Subsequent calculations use this lattice as a reference for the discretization of continuous surfaces. The attribute vector represents the pressure, $\boldsymbol{\pi}_k$, at a specific element of the matrix of the pressure vectors, $\boldsymbol{\Pi} = \bigcup_k \boldsymbol{\pi}_k$.

The pressure distribution patterns are analyzed for e.g., maximum pressure values, pressure gradient, and distance between areas of high pressures. These parameters are then statistically related to body properties and the angle of the pelvic tilt. The next step is to describe the pressure distribution data in fuzzy terms. This includes (i) the union, $\boldsymbol{\Pi}^F = \bigcup_i \boldsymbol{\Pi}_i^F$ $(i = 1, \ldots, N_S)$, of the pressure distribution measurements for N_S subjects sitting in a certain posture, for instance upright, and the conversion into a set of average pressure values, $\overline{\boldsymbol{\pi}}_k^F$ $(k = 1, \ldots, N_L)$ coupled with a set of metric/pressure occurrences, so that $\boldsymbol{\Pi}^F = \{\boldsymbol{\pi}_i^F, \varepsilon_i^F\}$ $(i = 1, \ldots, N_S)$, where N_L is the number of lattice points of the pressure distribution, and N_S is the number of subjects. This fuzzy pressure distribution is again represented as a number of percentiles in a statistical table.

4.3 Application of the flat pressure distribution on the unloaded body model

Applying the statistical set of flat pressure distributions, $\boldsymbol{\Pi}^F$, on the set of unloaded body shapes, $\mathbf{S}^0$, with FE techniques results in a corresponding set of deformed body shapes, $\mathbf{S}^F$. Since the maximum pressure, p_{max}, usually exceeds the physiologically acceptable maximum, a correction is needed.

4.4 The ideal pressure distribution

In the 'ideal' pressure distribution, $\boldsymbol{\Pi}^I$ the high pressure values are reduced until (i) a physiologically acceptable limit e.g., the level of decubitus (≈7 kPa [1]) and even lower pressure values in the medio-sagittal region, as far as possible, (ii) the curvatures of the lower closure do not exceed critical values, (iii) the existence of $\boldsymbol{\sigma}^0$, $\boldsymbol{\sigma}^1$ and $\boldsymbol{\sigma}^2$ singularities is minimized, and (iv) the average pressure is minimized (or the contact area maximized). It must be kept in mind that the $\boldsymbol{\Pi}^I$ also depends on the angle of the pelvic tilt. In forward rotated posture the main part of the upper body weight is transmitted via the upper legs depending on the sitting depth. In backward rotated posture the buttock areas (the area of the m. gluteus max) and possibly the coccyx are relatively more loaded. Thus each selected (statistical) subject and pelvic rotation put their own specific requirements for the $\boldsymbol{\Pi}^I$, and must be treated separately.

The basic idea is to achieve a stepwise correction on the flat pressure distribution data. Although from the comparison of the flat pressure distribution and the ergonomically acceptable pressure distribution we could get the implication on the maximum amount of the needed changes in the pressure distribution, the correction is carried out quasi-static, using finite steps to have control on the feasibility of the shape, since the pressure corrections may introduce unwanted shapes. The quantities that are modified by the stepwise correction have the indices $\ldots, n-1, n, n+1, \ldots$ The actual correction is achieved by two specific methods. The first one is called $dumb\ correction$ and the second $smart\ correction$. The dumb method is discussed first.

4.4.1 The theory of the dumb correction method

The first correction method is called 'dumb' because it is based only on fitting the intermediate pressure values to the ergonomically acceptable pressure distribution, $\boldsymbol{\Pi}^\varphi$. This is obtained by $\boldsymbol{\pi}_k^{n+1} = \boldsymbol{\pi}_k^n + a_k \boldsymbol{\pi}_k^n = \boldsymbol{\pi}_k^n (1 + a_k)$, where the pressure correction factor a_k is a positive or a negative scalar, depending on the required direction of the correction. Its calculation is given below.

Assume that (i) the flat pressure distribution $\mathbf{\Pi}^F = \{\boldsymbol{\pi}_k^F\}, \ (k = 1, \ldots, N_L)$, is measured, (ii) the average pressure $\overline{p} = \frac{1}{N_L}\sum_{k=1}^{N_L} \boldsymbol{\pi}_k^F$ has been calculated, and (iii) the distribution of the physiologically acceptable pressure distribution $\mathbf{\Pi}^\varphi = \{\boldsymbol{\pi}_k^\varphi\}$ is known. The dumb correction algorithm proceeds as follows.

i) Calculate the direction, d_k^n, of the pressure correction by $d_k^n = -(\boldsymbol{\pi}_k^n - \boldsymbol{\pi}_k^\varphi)/ \mid \boldsymbol{\pi}_k^n - \boldsymbol{\pi}_k^\varphi \mid$. If the calculated pressure $\boldsymbol{\pi}_k^n$ exceeds the physiologically acceptable level $\boldsymbol{\pi}_k^\varphi$ then $d_k = -1$, otherwise $d_k = +1$.

ii) Calculate the weights $w_k^n = (\boldsymbol{\pi}_k^n - \boldsymbol{\pi}_k^\varphi)/\sqrt{\sum_{k=1}^{N_L}(\boldsymbol{\pi}_k^n - \boldsymbol{\pi}_k^\varphi)^2}$. The weights determine the magnitude of the pressure steps, and include a normalization since the body weight is constant.

iii) Define the fraction α_0 which determines the magnitude of the correction steps as the inversion of the number of steps. The order of magnitude of the number of steps must be achieved by trials.

iv) Now the above mentioned pressure correction factor can be calculated as $a_k^n = \alpha_0 w_k^n d_k^n$.

v) Calculate the new pressure values according to $\boldsymbol{\pi}_k^{n+1} = (1 + a_k^n)\boldsymbol{\pi}_k^n$, which will be applied on the current body model. If $A_{(n)}$ is a square matrix with diagonal elements equal to $(1 + a_k^n), \ (k = 1, \ldots, N_L)$ and zero otherwise, and $\mathbf{\Pi}_{(n)} = (\boldsymbol{\pi}_1^n, \ldots, \boldsymbol{\pi}_{N_k}^n)^T$ then $\mathbf{\Pi}_{(n+1)} = A_{(n)}\mathbf{\Pi}_{(n)}$.
A further boundary condition is that on the boundary of the contact domain the pressure must be zero, $\boldsymbol{\pi} = 0$, and in a large enough neighbourhood the surface interpolating pressure distribution value points should be smooth.

4.4.2 The theory of the smart correction method

The *smart correction* method reasons about the pressure changes, the emerging shape features, the change of the local curvature (which leads to the appearance of sharp and phantom singularities), furthermore it considers the magnitude of the contact area. In order to explain the method we first have to introduce the following terms.

4.4.3 Merits and penalties

The successively calculated pressure distributions show their specific value with respect to the pressure $\mathbf{\Pi}^\varphi$ as well as the shape features. This value will be quantified by a specific quantity, M. If $M > 0$ then it is called merit, and if $M < 0$ then it is called penalty.[1]. The process tries to maximize M.

For each calculated M the lower closure of the currently available point cloud must be derived and analysed to reveal the shape features that influence sitting comfort, and therefore contribute to M. This issue will be further detailed below.

- The quantity M regarding the pressure values is defined as

$$M^{\mathbf{\Pi}} = b^{\mathbf{\Pi}} \sum_{k=1}^{N_L} \left(-\frac{\boldsymbol{\pi}_k - \boldsymbol{\pi}_k^\varphi}{\boldsymbol{\pi}_k^\varphi} \right) \tag{1}$$

  where $b^{\mathbf{\Pi}}$ is a weight. If $\boldsymbol{\pi}_k > \boldsymbol{\pi}_k^\varphi$ then M is a penalty and vice versa.

- The quantity M regarding the surface curvature, $\boldsymbol{\kappa} = \rho^{-1}$ (ρ is the radius of the curvature), is defined as

$$M^{\boldsymbol{\kappa}} = f(\boldsymbol{\kappa}_x) + f(\boldsymbol{\kappa}_x) \tag{2}$$

  where $f(\boldsymbol{\kappa})$ is a monotonously decreasing function. For increasing curvature, i.e. decreasing radius, M runs from merit to penalty, see figure 3a.

- The quantity M regarding sharp singularities is defined as

$$M^{\sigma_s} = b^{\sigma_s} \sum_{k=1}^{N_L} \left(\chi_s - \max \left| \left(\frac{e_1}{e_2} \right) \right|_{j=1,\ldots,N_L} \right) \tag{3}$$

  where e_1 and e_2 are obtained via the three-point test [18], see figure 3b. The value of χ_s has to be related to the average size of the point distances, for instance 10%, or 0.1. The factor b^{σ_s} is the weight for sharp singularities.

---

[1] The idea of awarding merits and penalties to the succeeding solutions in an iterative process was inspired by the TEX professional typesetting system that has been developed by D. Knuth [26].

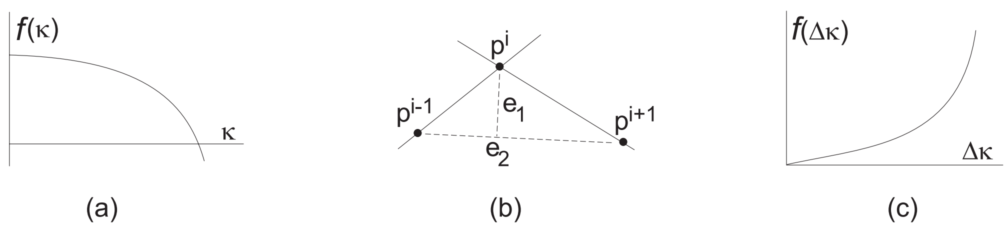

Fig 3. The weighting for curvature and phantom singularities, and a visualization of the three-point test for recognizing sharp singularities.

- The quantity M regarding phantom singularities is defined as

$$M^{\sigma_p} = b^{\sigma_p} \sum_{k=1}^{N_L} (\chi_p - f(|\Delta\boldsymbol{\kappa}_k|)) \tag{4}$$

  where $\Delta\boldsymbol{\kappa}$ is the distance of the jump of the centres of the curvatures within the singularity-area. The factor b^{σ_p} is the weight factor for phantom singularities. If a sudden change of the curvature exists, then M becomes a strong penalty, see figure 3c.
- The quantity M regarding the average pressure is defined as

$$M^{\overline{p}} = b^{\overline{p}}(1 - \overline{p}/\overline{\overline{p}}^F) \tag{5}$$

  The $\overline{\overline{p}}^F$ is the average pressure of all subjects sitting in the same position. The index F refers again to a flat surface.
- The totalled M is calculated as

$$M = M^{\boldsymbol{\Pi}} + M^{\boldsymbol{\kappa}} + M^{\sigma_s} + M^{\sigma_p} + M^{\overline{p}} \tag{6}$$

4.4.4 The procedure of the smart correction

Below we turn our attention to the smart pressure correction algorithm. This method uses the partial derivatives of M with respect to pressure:

$$\nabla M = \left(\frac{\partial M}{\partial \boldsymbol{\pi}_1}\mathbf{e}_1, \ldots, \frac{\partial M}{\partial \boldsymbol{\pi}_{N_k}}\mathbf{e}_{N_k} \right) \tag{7}$$

where $\mathbf{e}_i$ is the unit vector along the $\boldsymbol{\pi}_i$-axis. The partial derivatives are estimated by

$$\frac{\partial M}{\partial \boldsymbol{\pi}_k} = \frac{M(\boldsymbol{\pi}_k + \alpha'(\alpha_0 \boldsymbol{\pi}_k)) - M(\boldsymbol{\pi}_k)}{\alpha'(\alpha_0 \boldsymbol{\pi}_k)} \tag{8}$$

The factor α' is added to reduce the step α_0, and should be a reasonable small value e.g., 10%. The dimensionless gradient, Γ, equals

$$\boldsymbol{\Gamma} = \frac{\nabla M}{\sqrt{\sum_{k=1}^{N_k} \left(\frac{\partial M}{\partial \boldsymbol{\pi}_k}\right)^2}} \tag{9}$$

The direction of steepest ascent is the direction of $\boldsymbol{\Gamma}$. Thus the corrected pressure value equals $\boldsymbol{\pi}_k^{n+1} = \boldsymbol{\pi}_k^n + \alpha_0(\boldsymbol{\Gamma}_k)^T \Delta p$, where Δp has to be determined by trial and error-procedure. A good starting value can be $\Delta p = 0.1 \max(p_k - p_k^{\varphi})$

Now the actual steps of the compensation procedure will be explained.

A. $\boldsymbol{\Pi}^F$ is applied by the FE engine on Ξ^0. This results in a modified point cloud, Ξ^F, showing a more or less flat lower closure $\boldsymbol{\Lambda}^F$.
B. Calculate M for Ξ^F and $\boldsymbol{\Pi}^F$.
C. Apply the dumb correction algorithm, after which $\boldsymbol{\Pi}_{(n=1)} = (A^F)\boldsymbol{\Pi}^F$. This results in $\Xi_{(n=1)}$.
D. Calculate $M_{(n=1)}$.
E. Calculate ∇M.

F. Now the smart correction is applied $\Delta\mathbf{\Pi}_{(n)} = \mathbf{\Pi}_{(n)} + \alpha_0 \mathbf{\Gamma}^T_{(n)} \Delta p$

G. Calculate $M_{(n)}$ $(n = 2, 3, \ldots)$ and $\Delta M = M_{(n-1)} - M_{(n)}$.

H. If $| \Delta M | < \varepsilon$, where ε must be experimentally 'learned', then stop the iterative process, otherwise go to D.

The result of this procedure for all statistical subjects and properties is a set of N_P point clouds Ξ^I, where N_P is the number of pressure distribution percentiles of the pressure distribution table. The next steps concern the generation of the actual continuous surface for input to physical prototyping techniques.

5 SURFACE CONSTRUCTION

In order to construct the physical surfaces that are suited for rapid prototyping the point sets, $\mathbf{\Xi}^I_{ij}$ $(i = 1, \ldots, N_S; j = 1, \ldots, N_P)$, that were derived above for each statistical subject and pressure percentile, are now converted via (i) the detection of the lower closures, (ii) the detection of singularities, (iii) the representation by natural surfaces with corresponding singularities, (iv) the decomposition into synthetic surfaces, and (v) the formation of fitted surfaces. This has been described in detail in [18, 23]. Below we give a short summary.

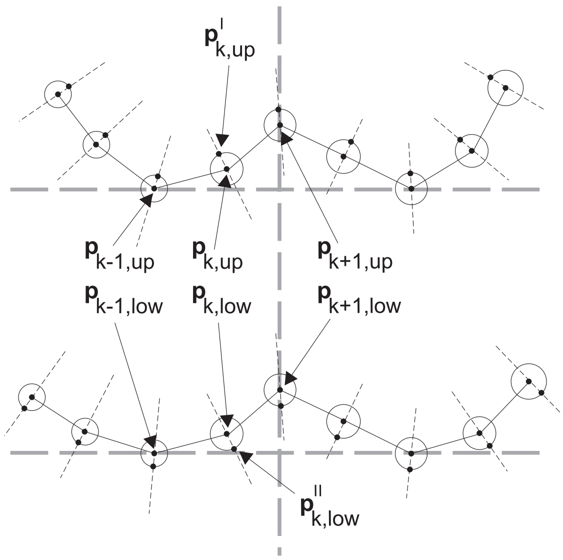

Fig 4. The closure operation

The surface construction starts with the determination of the upper and lower closures of the lower boundary of the point cloud $\Xi^I = \{\mathbf{p}_k\}$, see figure 4. The two grey horizontal dashed lines coincide. The vertical one indicates the projection of the midpoint of the ischial tuberosities. The double primed points, $\mathbf{p}'$ and $\mathbf{p}''$, will be used to construct the metric occurrences of the fuzzy surface.

5.1 Surface construction

From the resulting point cloud a physical surface must be constructed. In general a physical surface consists of one or more natural surfaces ω_i and the corresponding shape singularity $\boldsymbol{\sigma}_i$. A natural surface is a C^2-continuity manifold of dimension 2; it contains thus even no phantom singularities. It seems reasonable to expect that the resulting sitting surface consists of at least three natural surfaces, ω_1, ω_2 and ω_3, see figure 5.

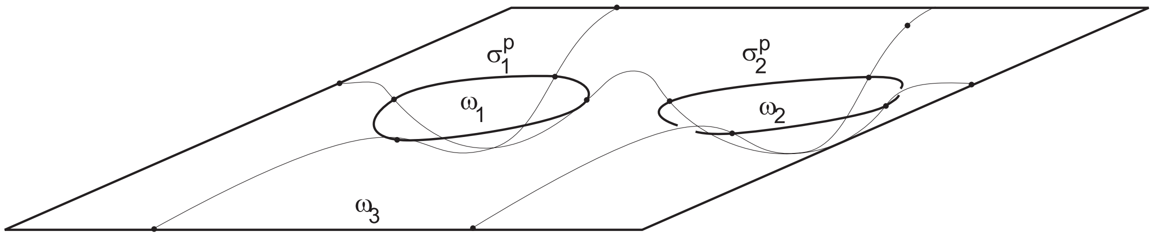

Fig 5. The expected features of the 'physical sitting surface'

The surface ω_1 is connected to ω_2 and ω_3 by the phantom cyclic singularities $\boldsymbol{\sigma}_1^p$ and $\boldsymbol{\sigma}_2^p$.
The actual surface construction contains the following steps.

(i) The boundary points are recognized by their 'connectedness'. Along the boundary the number of connections with the metric occurrence of a point with the metric occurrences of its neighbouring points is drastically reduced if the point is a member of the boundary of the surface. This fact can be used as a criterion for being a boundary point. This procedure is also used to detect holes within a surface.

(ii) Recognition of singularities. Let the point $\{\mathbf{p}_p\}$ be a singularity point of the manifold M. Let U be a small environment of $\mathbf{p}_k$. Three different types of singularities are considered. Zero order or spike singularities at $\mathbf{p}_k$ require that $(U \cap M) - \mathbf{p}_k$ is a C^2 M^2. First order or crest singularities require that $(U \cap M) - \{\mathbf{p}_k\}$ consists of two $C^1G^0M^2$ and $\{\mathbf{p}_k\}$ is a C^1 M^1. Second-Order or phantom singularities require that $(U \cap M) - \{\mathbf{p}_k\}$ consists of two G^2M^2 and $\{\mathbf{p}_k\}$ is a C^1M^1. The second order singularity shows a continuous tangent space.

(iii) After the recognition of the boundary, the holes and the singularities, the physical surface $\boldsymbol{\phi}$ can be constructed and represented as a set of natural surfaces, $\boldsymbol{\omega}_i$, which by their definition contain no singularities, and singularities, $\boldsymbol{\sigma}_i$, so that $\boldsymbol{\phi} = (\cup\boldsymbol{\omega}_i) \bigcup (\cup\boldsymbol{\sigma}_i)$

(iv) The natural surfaces are decomposed into a set of synthetic surfaces e.g., four sided surface patches. A synthetic surfaces is an analytical set.

(v) Then, for prototyping purpose, the continuous surfaces are estimated by interpolation techniques, such as least squares fitting to a function, variational techniques, or spline fitting.

(vi) The resultant surface is checked for ergonomically smoothness requirements, and for singularities. Then the designer can apply further refinements, surface rendering, and visualization of the surface.

(vii) The final surface is now ready for prototyping. This subject is discussed extensively in [27].

6 USER TRIALS

In figure 1 the rectangle with *USER TRIALS* is given extra weight. The reason is that user trials are always required to judge the quality of the product in practice. The outcome of such trials gives increased understanding of the relationships of shape, functionality and the ergonomical qualities such as comfort and effectivity. Possible troubles should be converted to improved ergonomical pressure and shape guidelines and requirements.

7 CONCLUSIONS

A system of methods and algorithms was developed, that uses ergonomics data to construct a FE model of the human pelvic area, and that applies pressure distribution data, measured on a flat supporting surface, on the FE model. This gives a point cloud with a more or less flat lower closure. This closure is converted to an 'ideal' shape. The final step is then to derive the real physical surface definition for physical prototyping.

The conversion is a iterative, *self learning* process, which resembles strongly the perceptron model from the area of artificial neural networks.

Initially, each step should be judged by the designer of the product which is, in this context, sitting supports. Furthermore, the area of user trials must never be omitted. From the ergonomics point of view the user trial constitute the very basis for the final decision whether the surface is acceptable or not. Of course, many important design aspects are not included in this manuscript, such as aesthetics, manufacturability or constructional properties. These form other conceptual designs to be included in a comprehensive computer based artificial knowledge system [28].

Other aspects that were not discussed relate to the mechanical properties of the sitting surface, for instance the influence of a backrest, arm rests, and the hardness of the support. Especially in automobiles the seats are usually not designed in modules for specific user groups, so that a certain seat is used by a broad class of individuals.

Future research includes the further development of the algorithms, the actual construction of FE models based on real human data, and the quantification of the weights of the assessment of merits and penalties.

References

[1] DA Hobson. *Contributions of posture and deformity to the body-seat interface conditions of a person with spinal cord injuries*. PhD thesis, University of Strathclyde, Glasgow, Scotland, 1988.

[2] CCM Moes. The Sitting Pressure Distribution and Pressure Gradient. Article in preparation.

[3] I Horváth, JS Vergeest, Z Rusák, and A Kooijman. Fuzzified Geometric Model to Support Conceptual Design: mathematical and Methodological Fundamentals. In *Proceedings of the ICED*, München, august 24–26 1999.

[4] I Horváth and JSM Vergeest. Natural Representation of Shapes with Singularities. *Intern. J. of Shape Modeling*, 3(3&4):127–140, 1998.

[5] RHM Goossens. *Biomechanics of Body Support*. PhD thesis, Erasmus Universteit, Rotterdam, the Netherlands, 1994.

[6] M Kosiak. Etiology of decubitus ulcers. *Archives of Physical and Medical Rehabilitation*, 42:19–29, 1985.

[7] JC Barnebel. Pressure management. *Prosthetics and Orthotics International*, 15:225–231, 1991.

[8] NR Reddy, V Palmieri, and GvB Cochran. Subcutaneous interstitial fluid pressure during external loading. *Am. J. Physiol.*, 240:R327–R329, 1981.

[9] JFM Manschot and AJM Brakkee. Characterization of in vivo mechanical skin properties independent of measuring configuration. *Bioengineering and the Skin*, 3:1–10, 1987.

[10] EM Landis. Micro injection studies of capillary blood pressure in human skin. *Heart*, 15:209–228, 1930.

[11] L Zhang, MG Helander, and CG Drury. Identifying Factors of Comfort and Discomfort in Sitting. *Human Factors*, 38(3):377–389, 1996.

[12] M Zhang, YP Zheng, and ATF Mak. Estimating the effective young's modulus of soft tissues from indentation tests – nonlinear finite element analysis of effects of friction and large deformation. *Med. Engin. Phys.*, 19(6):512–517, 1997.

[13] HAM Staarink. *Sitting Posture, Comfort and Pressure*. PhD thesis, Delft University of Technology, Delft, the Netherlands, 1995.

[14] NP Reddy, H Patel, and GVB Cochran JB Brunski. Model experiments to study the stress distributions in a seated buttock. *J. Biomechanics*, 15(7):493–504, 1982.

[15] WW Chow and EI Odell. Deformations and Stresses in Soft Body Tissues of a Sitting Person. *Journal of Biomedical Engineering*, 100(may):79–87, 1978.

[16] CCM Moes. Measuring the tilt of the pelvis. *Ergonomics*, 41(12):1821–1831, 1998.

[17] SP Levine, RL Kett, and M Ferguson-Pell. Tissue Shape and Deformation Versus Pressure as a Characterization of the Seating Interface. *Assistive Technology*, 2(3):93–99, 1990.

[18] I Horváth and JSM Vergeest. Theoretical Fundamentals of Natural Representation of Shapes Generated with Gestural Deveces. In I Horváth and A Taleb-Bendiab, editors, *Proceeding of the 2nd Int. Symp. on TMCE*, pages 393–409, Manchester, UK, 21–23 april 1998.

[19] I McClelland. Product assessment and user trials. In Wilson and Corlett [20], pages 249–284.

[20] JR Wilson and EN Corlett, editors. *Evaluation of Human Work*, London, 1995. Taylor & Francis.

[21] WM Krogman and MY İşcan. *The Human Skeleton in Forensic Medicine*. Charles C Thomas, Springfield, Illinois, USA, 1 edition, 1986.

[22] CCM Moes. The Angle of the Pelvic Tilt,. article in preparation.

[23] CCM Moes and I Horváth. Consideration of Pressure Distribution in Conceptualization of the Shape of Body Supports. In *Proceedings of the International Conference on Engineering Design ICED '99*, Munich, Germany, 1999. in press.

[24] CCM Moes and I Horváth. Ergonomics considerations for the conceptualization of the shape of body supports. In *Proceedings of the 6th CIRP Conference on Computer Aided Design*, Enschede, the Netherlands, 1999.

[25] CCM Moes and CMJ van Hulten. The dynamical assessment of pressure distribution on bicycle saddles. In GPH Hermans and WL Mosterd, editors, *Proceedings of the XXIV World Congress of Sports Medicine*, pages 797–801, Amsterdam, May 27–June 1 1990. Exerpta Medica.

[26] DE Knuth. *The TEXbook*, volume A of *Computers and Typesetting*. Addison Wesley, 1986.

[27] I Horvath, JSM Vergeest, JJ Broek, and A de Smit. Tool Profile and Tool Path Calculation for Free-form Thick layered Fabrication. *Computer Aided Design*, 40(14):1097–1110, 1998.

[28] I horváth. Shifting Paradigms of Computer Aided Design. Technical report, Delft University of Technology, Faculty of Industrial Design Engineering, 1998. Inaugural Speech.